JACS JOURNAL OF THE AMERICAN CHEMICAL SOCIETY

pubs.acs.org/JACS

Article

# Co(III)/Alkali-Metal(I) Heterodinuclear Catalysts for the Ring-Opening Copolymerization of $CO_2$ and Propylene Oxide

Arron C. Deacy, Emma Moreby, Andreas Phanopoulos, and Charlotte K. Williams*

Cite This: J. Am. Chem. Soc. 2020, 142, 19150−19160

Read Online

ACCESS | Metrics & More | Article Recommendations | Supporting Information

**ABSTRACT:** The ring-opening copolymerization of carbon dioxide and propene oxide is a useful means to valorize waste into commercially attractive poly(propylene carbonate) (PPC) polyols. The reaction is limited by low catalytic activities, poor tolerance to a large excess of chain transfer agent, and tendency to form byproducts. Here, a series of new catalysts are reported that comprise heterodinuclear Co(III)/M(I) macrocyclic complexes (where M(I) = Group 1 metal). These catalysts show highly efficient production of PPC polyols, outstanding yields (turnover numbers), quantitative carbon dioxide uptake (>99%), and high selectivity for polyol formation (>95%). The most active, a Co(III)/K(I) complex, shows a turnover frequency of 800 $h^{-1}$ at low catalyst loading (0.025 mol %, 70 °C, 30 bar $CO_2$). The copolymerizations are well controlled and produce hydroxyl telechelic PPC with predictable molar masses and narrow dispersity ($Đ$ < 1.15). The polymerization kinetics show a second order rate law, first order in both propylene oxide and catalyst concentrations, and zeroth order in $CO_2$ pressure. An Eyring analysis, examining the effect of temperature on the propagation rate coefficient ($k_p$), reveals the transition state barrier for polycarbonate formation: $\Delta G^{‡}$ = +92.6 ± 2.5 kJ $mol^{-1}$. The Co(III)/K(I) catalyst is also highly active and selective in copolymerizations of other epoxides with carbon dioxide.

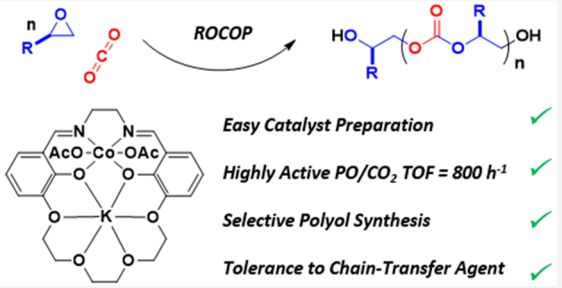


## INTRODUCTION

Carbon dioxide utilization is a grand challenge for contemporary chemistry, and although several efficient reactions are known, few are viable or true utilizations when considered more broadly.[1,2] Many require esoteric, greenhouse gas emitting, and expensive stoichiometric reagents, while others yield products with no current large-scale application, or need unacceptably high catalyst loadings or operate under conditions, including carbon dioxide purity, incompatible with scale-up.[3] In contrast, epoxide and carbon dioxide ring-opening copolymerization (ROCOP) is well suited for large-scale deployment since it applies already commercial monomers, enables significant carbon dioxide sequestration, and produces valuable polymers whose properties allow for the replacement of existing petrochemicals.[3−5] This process can sequester up to 50 wt % carbon dioxide into the polymer and it is truly catalytic allowing for multiple turnovers and high converson of epoxide.[3−5] At the cutting-edge are carbon dioxide and propylene oxide derived polyols which are low molar mass, hydroxyl end-capped polypropylene carbonate (PPC) or polyethercarbonates. These polyols are applied to make polyurethanes to construct mattresses and furniture foams, insulation sheet foam, coatings, sealants, and elastomers.[4,6−8] Life-cycle assessment shows that polyols with just 20 wt % $CO_2$ content (i.e., imperfectly alternating polymers) display a ∼20% reduction in green-house gas emissions and fossil fuel consumption compared to currently used petrochemicals.[9] High molar mass polycarbonates are also explored as toughened plastics, elastomers, and adhesives.[10] In terms of polyols, the use of propylene oxide as the epoxide is particularly important because it is an inexpensive commodity chemical already used at large-scale in polyol manufacture,[11] and it delivers attractive material properties.[4,6−8] While tremendous advances have been made in high molar mass PPC catalysis,[12−24] the production of the desired low molar mass polyols from propylene oxide and carbon dioxide is challenging.[4,25,26] One difficulty is that any catalyst must tolerate a large excess of the protic starter or chain transfer agent (CTA), typically a diol or diacid, essential to control the chain end-group chemistry and ensure that polyols achieve the correct molar mass, even at high epoxide conversions (Figure 1).[4]

Among the most active high molar mass PPC catalysts are cobalt(III) salen complexes, [(salen)Co(III)X] where X = carboxylate or halide, and these compounds are best applied with an equimolar quantity of an ionic cocatalyst, typically

Received: August 3, 2020
Published: October 27, 2020







https://dx.doi.org/10.1021/jacs.0c07980
J. Am. Chem. Soc. 2020, 142, 19150−19160

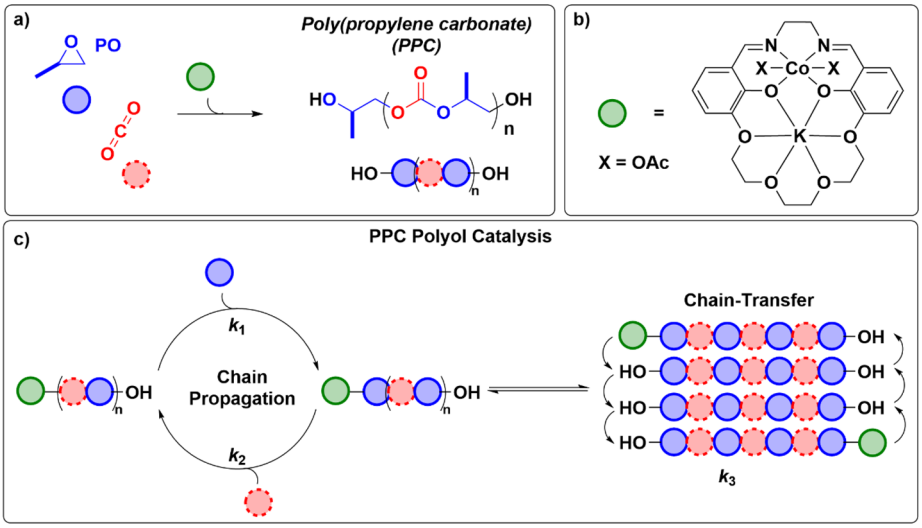


**Figure 1.** (a) $PO/CO_2$ ROCOP to make poly(propylene carbonate) (PPC) polyols. (b) Illustration of one of the heterodinuclear catalysts used in this investigation (2). (c) Catalytic cycle for $PO/CO_2$ ROCOP illustrating both propagation and chain transfer reactions (epoxide ring-opening $k_1$, $CO_2$-insertion $k_2$ and chain-transfer $k_3$).

bis(triphenyl phosphine)iminium chloride (PPNCl).[12−21] Although this type of catalyst can be used to prepare polyols, they usually show significantly compromised activity. For example, [(salen)CoX]/PPNX shows an activity, TOF, of just 10 $h^{-1}$ when applied with the added water (as CTA) necessary to selectively produce polyols.[26] Another problem is the use of PPNX salts which are toxic, expensive, poorly soluble in many epoxides, and may be corrosive to steel. As the active catalyst comprises an ion pair, rapid deactivation occurs at the necessary low catalyst loading, which is another detraction.[14,15] To address these limitations, Nozaki and co-workers, and subsequently many others, reported modified [(salen[$NR_3^+$])-Co(III)X]X′ complexes, i.e., single component catalysts, where the salen ligand is modified to include a covalently bonded organic salt cocatalyst, most commonly an ammonium salt.[12,14,15,18] These catalysts show better turnover frequencies for low molar mass PPC, for example, achieving a TOF of 48 $h^{-1}$ with excess methanol.[18] Detailed optimization resulted in a catalyst featuring four ammonium "arms", [(salen[$NBu_3^+$]$_4$)-Co(III)(OAc)]($NO_2^-$)$_4$, that achieved an impressive TOF of 10 300 $h^{-1}$ (0.001 mol % catalyst, 80 °C, 20 bar $CO_2$) and importantly is stable to copious quantities of CTA (400 equiv).[27] Unfortunately, this catalyst is somewhat complex to prepare, requiring >8 synthetic steps, and has an ill-defined composition and unclear mechanism.[28,29] Very recently, the tethered cocatalyst strategy also significantly improved an Al(III)-porphyrin catalyst, but for $CO_2$/CHO ROCOP.[30]

Lewis acid−base pair catalysts, of the form $Et_3B$/*tetra*-butylammonium carbonate (TBAC), also successfully yielded PPC polyols, although with low TOF = 3 $h^{-1}$ and requiring high catalyst loading (7.5 mol % $BEt_3$, 2.5 mol % TBAC, 40 °C, 10 bar).[31] Recently, recycling of this catalyst system has been reported with >95% catalyst recovery.[32] The stratagem of tethering the Lewis acid−base pair has significantly enhanced rates for $CO_2$/CHO ROCOP, but there are not yet reports of these catalysts for PPC polyol synthesis.[33]

Homogeneous dinuclear metal ROCOP catalysts operate without cocatalyst, show high activity and selectivity at low carbon dioxide pressures for CHO/$CO_2$ ROCOP, and retain performances when using chain transfer agents to selectively deliver PCHC polyols.[34−46] The most active are heterodinuclear catalysts which show synergy in CHO/$CO_2$ ROCOP.[43−49] Nonetheless, so far these dinuclear catalysts underperform in propylene oxide (PO)/carbon dioxide ROCOP: they either scarcely turnover to PPC or produce cyclic carbonate.[34,38,43] Motivated by the heterodinuclear synergy concept, this study targets heterodinuclear $PO/CO_2$ ROCOP catalysts. The catalyst selection is underpinned by the following guidelines: (1) The optimum internuclear separation should be ∼3−4 Å to provide for intermetallic "cooperation" in the ring-opening transition state and intermediate.[35,40,45,50] (2) The chain-shuttling mechanism, operative for other dinuclear catalysts, is accelerated by trans- disposed coligands and chain growth alternating between the two metals.[34−36,38,43−45] (3) For CHO/$CO_2$ ROCOP, the most effective metal combinations feature M(II)M′(II), where M = Co(II) and M′ = Mg(II).[43] Here, $PO/CO_2$ ROCOP, catalysts of the form M(III)/M′(I), where M = Co(III) and M′ = Na, K, Cs, Rb(I), are proposed to exploit the high nucleophilicity of Co(III)-propylene carbonate intermediates and the oxophilicity of Group 1 metals toward epoxide coordination. Additionally, Group 1 metals are attractive due to their abundance, low cost, lack of color, and low toxicity. Heterodinuclear complex formation is essential since prior work has established that ROCOP using mixtures of [(salen)Co(III)X] complexes and Group 1 crown ether additives yielded cyclic carbonates.[13] To make the heterodinuclear M(III)/M(I) complex, a macrocyclic ligand featuring differentiated binding cavities was selected, with a tetradentate Schiff base to coordinate the Co(III) and a "crown-ether" moiety for M(I) (Figure 2). The ligand features two bridging phenolate sites which could enhance electronic communication between Co(III) and M(I), which may increase electronic synergy in catalysis (Figure 1a).[34,36,43] Related transition metal/M(I) heterodinuclear complexes are successful magnetic resonances probes (Co(II)/Na(I)), CH oxidation catalysts (Fe(III)/K(I)), and epoxidation catalysts (Mn(III)/Na(I)).[51−56]


https://dx.doi.org/10.1021/jacs.0c07980
J. Am. Chem. Soc. 2020, 142, 19150−19160

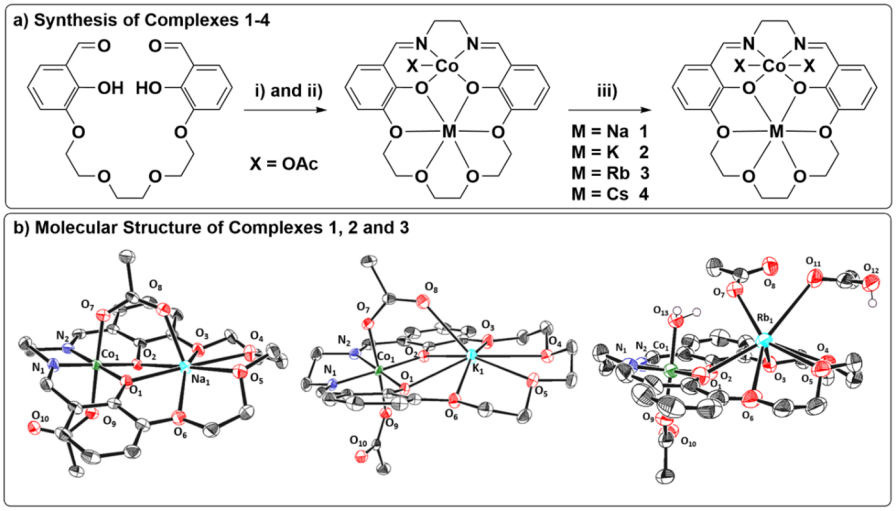


**Figure 2.** (a) Synthesis of the heterodinuclear complexes **1**−**4**. Reagents and conditions: (i) M(OAc) [M = Na, K, Rb, or Cs], $Co(OAc)_2$, MeCN, 25 °C, 30 min, $N_2$. (ii) Ethylenediamine, MeCN, 25 °C, 16 h, $N_2$. (iii) AcOH (2 equiv), MeCN, air, 72 h, >50% yield. (b) ORTEP representation of the molecular structures of complexes **1**−**3**, with hydrogen atoms and residual solvents omitted for clarity, and thermal ellipsoids are represented at 50% probability (see SI for experimental details).

## RESULTS AND DISCUSSION

Complexes **1**−**4** were synthesized from the macrocycle ligand (SI for ligand synthesis) by the addition of an equivalent of the appropriate alkali-metal(I) acetate, followed shortly after by the addition of an equivalent of cobalt(II) acetate. The reaction mixture was stirred for 30 min, at 25 °C, and then ethylenediamine was added and the solution stirred for a further 16 h. The resulting solution was exposed to air and two equivalents of acetic acid added to oxidize the Co(II) center. The resulting Co(III)/M(I) complexes were isolated in >50% overall yield as pale brown solids. The complexes were characterized by NMR spectroscopy (Figure S2−S10), mass spectrometry (Figure S11−S13), IR spectroscopy (Figure S14), elemental analysis, and where possible, by single crystal X-ray diffraction (SI for details). For example, the NMR spectrum of **1** shows the disappearance of the phenolic protons, at ∼10.86 ppm in the free ligand, and the appearance after complexation of both ethylene ($^1$H: 4.31; $^{13}$C: 59.4 ppm) and acetate ($^1$H: 1.45; $^{13}$C: 179.5, 24.8 ppm) resonances, respectively. The transformation of the aldehyde to imine functional groups results in shifting of a singlet resonance from 9.94 to 7.70 ppm in the $^1$H NMR spectrum. During the synthesis, both metals are added in short succession and yet there is selective formation of the heterodinuclear complex. This arises because the ligand binding "pockets" discriminate between the metals' coordination chemistry and ionic radii (Co(II) = 0.75 Å, Na(I) = 1.1 Å, K(I) = 1.5 Å, Rb(I) = 1.6 Å and Cs(I) = 1.7 Å vs binding sites $N_2O_2$ = 1.9 Å, 18C6 = 2.7 Å).[57]

The 2D DOSY NMR spectra show a single diffusion coefficient for complexes **1**−**4**, indicative of a single structure in solution (Figure S10). The solution hydrodynamic radii are 5.14, 5.17, 5.65, and 6.66 Å for **1**−**4**, respectively. For complexes **1** and **2**, values correlate well with those calculated from the solid state structures (vide infra) and indicate monomeric species. Complex **3** shows a smaller value (5.65 Å) than that calculated for the dimeric solid (6.45 Å) and correlates better to a "half-dimeric" structure (5.23 Å) suggesting it is monomeric in solution. Although the solid state structure of complex **4** was not obtained, its solution hydrodynamic radius (6.66 Å) falls in the expected range for a dimer. The change in complex nuclearity on descending Group 1 can be rationalized by increasing larger radii, e.g., of Rb(I) and Cs(I), enabling access to higher coordination numbers and facilitating complex aggregation.[58]

The MALDI-ToF mass spectra display molecular ions, at 495, 511, and 604 amu, for complexes **1**, **2**, and **4**, respectively, and values correspond to the molecular cation, $[LCo(II)M]^+$ (Figure S11−S13). The isotope distribution patterns match those expected. Crystals suitable for single crystal X-ray diffraction were obtained via vapor diffusion of pentane (**1**) or diethyl ether (**2**) into a saturated solution of each complex in dichloromethane. Structural elucidation confirmed the desired heterodinuclear complexes (Figure 2b). Catalysts **1** and **2** are isostructural, as both are monomeric with an octahedral cobalt(III) coordinated in the bis(iminophenol) ligand cavity, and the alkali metal(I) coordinated in the crown ether cavity. There is a measurable increase in Co−M separation (M = Na; 3.388 Å, K; 3.698 Å) consistent with the increase in radii. In each structure, one acetate ligand bridges ($\kappa_2$) between the Co(III) and M(I) and the other is coordinated only to cobalt ($\kappa_1$). The structures of complexes **1** and **2** are formally cobalt "ate" species; i.e., the Co(III) is anionic while the M(I) is cationic.

Catalysts **1**−**4** were each tested in $CO_2$/PO ROCOP, at 50 °C, using neat PO (14 M, 6 mL), 0.025 mol % catalyst, 20 bar $CO_2$ pressure and 0.5 mol % 1,2-cyclohexane diol (i.e., 20 equiv CTA vs catalyst) to deliver PPC polyols (Table 1). Under these polyol synthesis conditions, all catalysts showed very good activity and resulted in near quantitative $CO_2$ uptake. The reactions were also highly selective with catalysts **2** and **3**, in particular, showing very little cyclic carbonate byproduct. In all cases, the poly(propylene carbonate) formed without detectable ether linkages and with molar mass values consistent with theoretical values and within the desired polyol range. The PPC polyols show monomodal, narrow dispersity distributions ($Đ$ < 1.10) with excellent selectivity for hydroxyl end-groups (vide infra).

Catalyst **2**, i.e., Co(III)K(I), is the most active and has a turnover frequency (TOF) of 340 $h^{-1}$ at 50 °C ($k_p$ = 11.20


https://dx.doi.org/10.1021/jacs.0c07980
J. Am. Chem. Soc. 2020, 142, 19150−19160

Table 1. ROCOP of $CO_2$/PO of Catalysts 1−4[a]

| # | Co(III)/M(I) | time (h) | conv. (%)[b] | $CO_2$ (%)[c] | polym. (%)[d] | TON[e] | TOF ($h^{-1}$)[f] | $k_p$ ($mM^{-1}$ $s^{-1}$)[g] | $M_n$ [Đ] (g $mol^{-1}$)[h] |
|---|---|---|---|---|---|---|---|---|---|
| 1 | Na = **1** | 5.0 | 15 | >99 | 79 | 600 | 120 | 2.09 | 2300 [1.08] |
| 2 | K = **2** | 4.0 | 34 | >99 | 98 | 1360 | 340 | 11.20 | 5900 [1.10] |
| 3[i] | K = **2** | 1.4 | 28 | >99 | 93 | 1120 | 800 | 24.0 | 5800 [1.07] |
| 4[j] | K = **2** | 19.8 | 90 | >99 | 98 | 1800 | 91 | 10.70 | 8800 [1.04] |
| 5 | Rb = **3** | 23 | 31 | >99 | 91 | 1240 | 54 | 1.77 | 6500 [1.07] |
| 6 | Cs = **4** | 23 | 27 | >99 | 84 | 1080 | 47 | 1.76 | 5600 [1.08] |
| 7[k,13] | [(salen)Co(2,4-DNP)]/18C6/KI | 3.0 | 27 | >99 | 41 | 540 | 182 | – | 4700 [1.43] |
| 8[l,26] | [(salcy)Co($O_2CCF_3$)]PPN($O_2CCF_3$) (20 equiv $H_2O$) | 48 | 95 | >99 | >99 | 475 | 10 | – | 7800 [1.06] |
| 9[m,18] | [(salen[$Pip^+$]$_2$)Co($OAc)_2$] (20 equiv MeOH) | 20 | 95 | >99 | 96 | 960 | 48 | – | 5100 [1.06] |
| 10[n,27] | [(salen[$NBu_3^+$]$_4$)Co(OAc)]$(NO_2)_4$ (400 equiv adipic acid) | 1 | 10 | >99 | >99 | 10 300 | 10 300 | – | 2600 [1.05] |
| 11[o,31] | $Et_3B$:[$NBu_4^+$]$_2$[$O_3C^{2-}$] | 14 | 95 | 91 | 95 | 37 | 3 | – | 4100 [1.10] |
| 12[p,59] | Zn-Co-DMCC (15 equiv sebacic acid) | 30 | 64 | 75 | 98 | 1280 g/g | 43 g/g/h | – | 1500 [1.10] |

[a]Reaction conditions: Catalyst (0.025 mol %, 3.5 mM), PO (6 mL, 14 M), 1,2-cyclohexanediol (0.5 mol %, 70 mM), 20 bar $CO_2$, 50 °C. [b]PO conversion determined from the relative integrals in the $^1$H NMR spectrum of PPC (4.92 ppm, 1H), PC (4.77 ppm, 1H), and PPO (3.46−3.64 ppm, 3H) using mesitylene as an internal standard (6.70 ppm). [c]$CO_2$ selectivity determined by the relative integrals in the $^1$H NMR spectrum of PPC (4.92 ppm, 1H) and PC (4.77 ppm, 1H) compared with PPO (3.46−3.64 ppm, 3H). [d]Polymer selectivity determined by the relative integrals in the $^1$H NMR spectra of PPC (4.92 ppm, 1H) against PC (4.77 ppm, 1H). [e]Turnover number (TON) = number of moles of PO consumed/number of moles catalyst. [f]Turnover frequency (TOF) = TON/time (h). [g]$k_p = k_{obs}/[cat]^1$; $k_{obs}$ determined as the gradient of the plot of $\ln[PO]_t/[PO]_0$ vs time. [h]Determined by GPC analysis, in THF, calibrated with narrow-$M_n$ polystyrene standards; dispersity values in parentheses. [i]Catalyst (0.025 mol %, 3.5 mM), PO (6 mL, 14 M), 1,2-cyclohexanediol (0.5 mol %, 70 mM), 30 bar $CO_2$, 70 °C. [j]Catalyst (0.05 mol %, 3.5 mM), PO (3 mL, 7 M), diethyl carbonate (3 mL), 1,2-cyclohexanediol (0.5 mol %, 70 mM), 20 bar $CO_2$, 50 °C. [k]Catalyst (0.05 mol %, 7.1 mM), PO (14 mL, 14 M), KI (0.05 mol %, 7.1 mM), 15 bar $CO_2$, 25 °C. [l]Catalyst (0.2 mol %, 10.0 mM), PO (0.5 mL, 4.6 M), toluene/chloroform (1 mL), PPNX (0.2 mol %, 10.0 mM), $H_2O$ (2.0 mol %, 1 M), 15 bar $CO_2$, 25 °C. [m]Catalyst (0.1 mol %, 7.2 mM), PO (1 mL, 7 M), 1,2-dimethoxyethane (1 mL), methanol (1.0 mol %, 0.14 M), 14 bar $CO_2$, 25 °C. [n]Catalyst (0.001 mol %, 1.7 μM), PO (12 mL, 14 M), adipic acid (0.4 mol %, 0.68 M), 25 bar $CO_2$, 75 °C. [o]Catalyst (7.5 mol %, 0.25 M, 1 mL from a 1 M THF solution), tetra-butyl ammonium carbonate (TBAC) (2.5 mol %, 0.09 M), PO (2 mL, 7 M), THF (1 mL), 10 bar $CO_2$, 40 °C. [p]Catalyst (50 mg), PO (100 mL, 14 M), sebacic acid (95 mmol, 0.95 M), 40 bar $CO_2$, 50 °C. For illustrations of the literature catalyst structures, see Figure S15.

$mM^{-1}$ $s^{-1}$, 98% PPC, 20 bar $CO_2$) which is increased to an impressive 800 $h^{-1}$ at 70 °C ($k_p$ = 24.0 $mM^{-1}$ $s^{-1}$, 93% PPC, 30 bar $CO_2$). Catalysts **1**, **3**, and **4** are all considerably less active ($k_p$ ∼ 2.00 $mM^{-1}$ $s^{-1}$) and selective than **2**.

The outstanding performance of the potassium heterodinuclear complex, compared to the other Group 1 metals, likely arises from a combination of carefully balanced metal sizes and binding affinities. When the alkali metal is too small, e.g., Na(I) in complex **1**, it may be coordinatively saturated by the macrocycle crown ether which hinders propylene oxide coordination. When the alkali metal is too large, e.g., Rb(I) or Cs(I) in complexes **3** or **4**, coplanar metal coordination within the macrocycle is no longer possible and aggregates form, as indicated by the DOSY NMR data. Catalyst **2** also produced PPC polyols with excellent productivity, reaching >90% conversion of PO while maintaining high activity and selectivity (Table 1, Entry 2). This data is significant since it demonstrates the ability to use these catalysts to fully convert the epoxide into the target PPC polyols.

Compared against other literature catalysts, the performance of **2** stands out. For example, Lu and co-workers reported a catalyst mixture of [(salen)Co(III)X] (X = 2,4-dinitrophenolate) with an equimolar amount of 18-crown-6/KI (1:1) which formed mostly cyclic carbonate (41% selectivity for PPC) with only half the activity of **2** and without any polyol formation (Table 1, Entry 7).[13] Compared against the [(salen)Co(III)-X]/PPNX system, applied under polyol formation conditions where X = trifluoroactetate, catalyst **2** shows >30× higher activity, at 10× lower loading.[26] As mentioned in the Introduction, the tethered catalyst [(salen[$Pip^+$]$_2$)Co($OAc)_2$] is less effective in polyol synthesis, with **2** showing 8× higher activity at 2× lower catalyst loading and delivering better selectivity.[18] Catalyst **2** is less active than the highly optimized tetra-ammonium substituted catalyst [(salen[$NBu_3^+$]$_4$)Co-(OAc)]$(NO_2)_4$, but is substantially higher yielding compared to the 10% PPC conversion reported.[27] Beneficially, **2** is fully characterized and does not contain any salts or anion mixtures.

Heterogeneous double metal cyanide catalysts are used industrially to produce poly(propylene oxide-ran-propylene carbonate) polyols—they show excellent activity but much lower carbon dioxide uptake (carbonate linkages <20%). Unfortunately these heterogeneous catalysts also produce significant quantities of cyclic carbonate byproducts (Table 1, Entry 12).[60,61] Wang and co-workers reported conditions, specifically at lower temperatures and using specific acidic cocatalysts and starters, that increase carbon dioxide uptake (% carbonate <75%). Nonetheless, these conditions impact negatively upon catalyst activity (TOF = 43 g/g/h, 15 equiv sebacic acid, 50 °C, 40 bar $CO_2$).[59] In comparison, **2** displays an equivalent activity (35 g/g/h at 50 °C), but, unlike the DMC catalysts, it may be applied at higher temperature without loss of selectivity. Thus, at 70 °C, its activity increases to 83 g/g/h without significant compromise in polymer selectivity.

Using low loadings of catalyst **2**, the molar mass of the resulting PPC was easily controlled by varying the amount of chain-transfer agent used (0−250 equiv, Table 2). When the catalyst was applied without CTA, the resulting PPC showed bimodal molar mass distributions attributed to chains which are catalyst initiated (lower MW series) and chains initiated


https://dx.doi.org/10.1021/jacs.0c07980
J. Am. Chem. Soc. 2020, 142, 19150−19160

**Table 2. Molecular Weight Control with Addition of Chain-Transfer Agent Using Catalyst 2**[a]

| # | CTA | conv. (%)[b] | $CO_2$ (%)[c] | polym. (%)[d] | TON[e] | $M_n$ exp CHD [OAc] (kg mol$^{-1}$)[f] | $M_n$ theoCHD + OAc (kg mol$^{-1}$)[g] | CHD:OAc[h] | $Đ$[i] |
|---|---|---|---|---|---|---|---|---|---|
| 1[j] | 0 | 21 | >99 | 93 | 840 | 33.7 [14.4] | 42.8 | 50:50 | 1.04 [1.10] |
| 2 | 5 | 58 | >99 | 94 | 5800 | 79.6 [38.9] | 84.5 | 76:24 | 1.06 [1.05] |
| 3 | 10 | 46 | >99 | 96 | 4600 | 36.8 [15.4] | 39.1 | 83:17 | 1.06 [1.08] |
| 4 | 20 | 52 | >99 | 97 | 5200 | 23.1 [10.7] | 26.5 | 95:05 | 1.03 [1.03] |
| 5 | 50 | 63 | >99 | 97 | 6300 | 12.3 | 12.9 | 99 | 1.06 |
| 6 | 100 | 69 | >99 | 94 | 6900 | 7.2 | 7.0 | 99 | 1.07 |
| 7 | 250 | 37 | >99 | 97 | 3700 | 1.3 | 1.5 | 99 | 1.16 |

[a]Reaction conditions: Catalyst (0.01 mol %, 1.9 mM), PO (15 mL, 14 M, 290 mmol), CTA = 1,2-cyclohexanediol, 20 bar $CO_2$, 50 °C. [b]PO conversion determined from the relative integrals in the $^1$H NMR spectrum of PPC (4.92 ppm, 1H), PC (4.77 ppm, 1H), and PPO (3.46−3.64 ppm, 3H) using mesitylene as an internal standard (6.70 ppm). [c]$CO_2$ selectivity determined by the relative integrals in the $^1$H NMR spectrum of PPC (4.92 ppm, 1H) and PC (4.77 ppm, 1H) compared with PPO (3.46−3.64 ppm, 3H). [d]Polymer selectivity determined by the relative integrals in the $^1$H NMR spectra of PPC (4.92 ppm, 1H) against PC (4.77 ppm, 1H). [e]Turnover number (TON) = number of moles of PO consumed/number of moles catalyst. [f]Determined by GPC analysis, in THF, calibrated with narrow $M_n$ polystyrene standards. [g]Theoretical molar mass determined by (TON × 102 g mol$^{-1}$)/number of initiators (CHD + OAc). [h]Determined by the relative ratios of the lower (OAc initiated) and upper (CHD initiated) molar mass distributions observed in GPC analysis. [i]Dispersity calculated by $M_w/M_n$. [j]0.025 mol % catalyst.

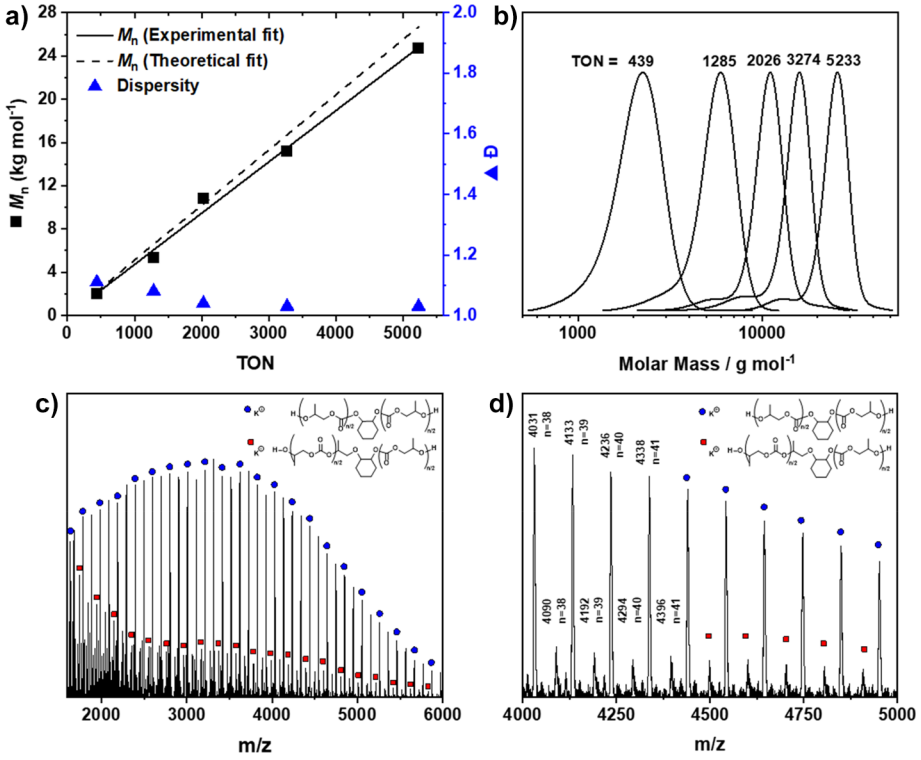


**Figure 3.** Polymerization data using catalyst **2** (Co(III)/K(I) for PO/$CO_2$ ROCOP (Table S1). (a) Plot of PPC molar mass ($M_n$: ■) and dispersity ($Đ$: ▲) versus turnover number (TON). (b) Evolution of the PPC molar masses showing an increase in molar mass (g mol$^{-1}$) with turnover number (TON) (note the low molar mass shoulder present in some cases arises from chains initiated from catalyst acetate groups). (c) MALDI-ToF spectrum (1000−6000 $m/z$) of poly(propylene carbonate) initiated from cyclohexanediol (●) and cyclohexane diol + one ether linkage (■). (d) Expanded region of the MALDI-ToF spectrum (4000−5000 $m/z$) showing both polymer distributions having a repeat unit of 102 g mol$^{-1}$ consistent with the value expected for poly(propylene carbonate).

from 1,2-propane diol (upper series, note the diol evolves by ring opening of epoxide and trace water as discussed previously[25]). For polymerizations conducted with progressively greater numbers of equivalents of CTA, the quantity of catalyst initiated polymer chains decreases resulting in the desired monomodal GPC traces when >50 equiv of CTA are used. The molar mass of the resulting polymers are progressively reduced as the quantity of CTA used increases, allowing access to PPC with controllable $M_n$ values spanning 79.6−1.3 kg mol$^{-1}$ correlating well with theoretical values.

Catalyst **2** shows excellent absolute performance and so a more detailed examination of polymerization control is warranted. The PPC is regiorandom as indicated by quantitative $^{13}$C{$^1$H} NMR spectroscopy with a head-to-tail proportion (HT) of 63% (Figure S16). A series of polymerizations conducted at systematically increasing catalyst loadings, from 0.05 to 0.01 mol % (Table S1), showed fast and highly selective catalysis in all cases and, as expected, allowed for good control over PPC molar mass. Plots of PPC molar mass vs turnover number (TON) are linear and there is close agreement between experimental and theoretical values.


https://dx.doi.org/10.1021/jacs.0c07980
J. Am. Chem. Soc. 2020, 142, 19150−19160

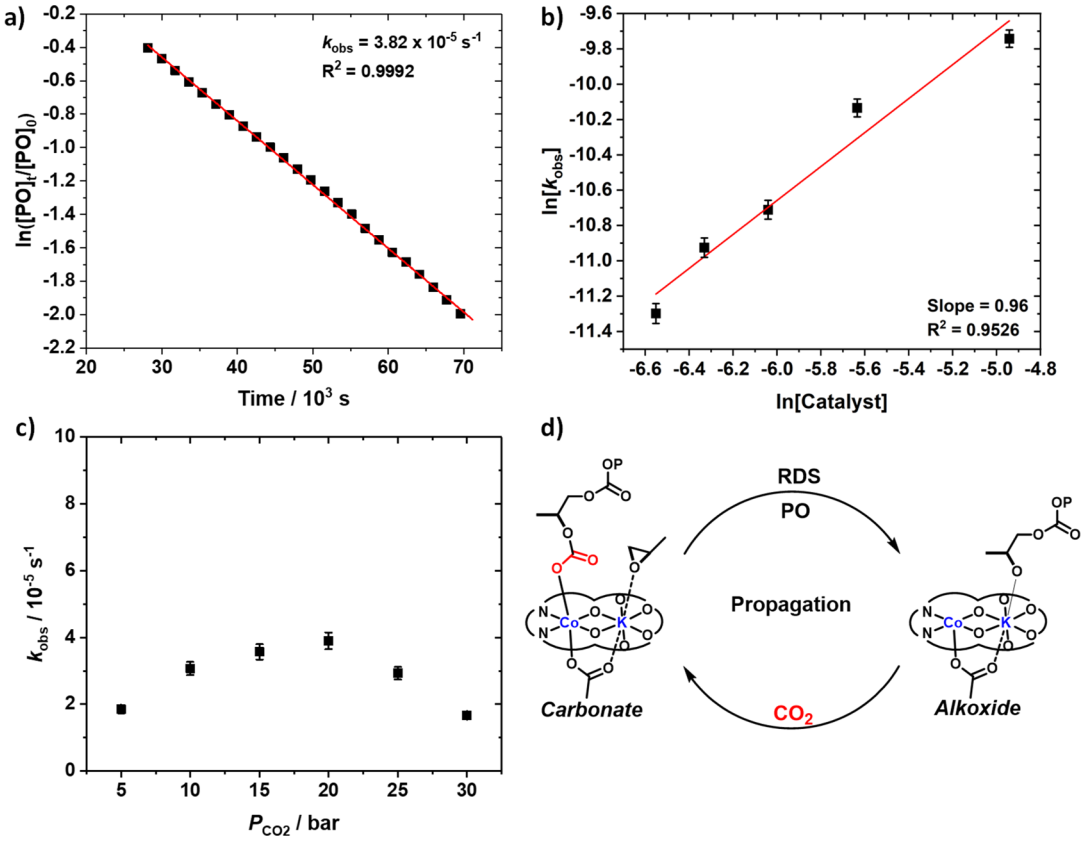


**Figure 4.** Kinetic data and pathway for catalyst **2** in PO/$CO_2$ ROCOP. (a) Semilogarithmic plot of $\ln[PO]_t/[PO]_0$ versus time (Table 1, Entry 4). (b) Plot of $\ln[k_{obs}]$ vs ln[**2**], where [**2**] = 1.56−7.13 mM (Table S1). (c) Plot of $k_{obs}$ vs $P_{CO_2}$ from 5 to 30 bar. (d) Illustration of polymerization pathway and rate-determining step. All errors are calculated from duplicate runs and there is an average error of ±5% on all data.

Both findings are consistent with controlled polymerizations, as are the observation that the molar mass distributions are monomodal, with consistently narrow dispersity values (Figure 3b). MALDI-ToF data show two distributions, both corresponding to PPC polyols and differing only in terms of one ether linkage. End group analysis, using $^{31}P\{^1H\}$ NMR spectroscopy, also confirms polyol formation (Figure 3c and d, Figure S17).

One puzzle for the previously reported [(salen)Co(III)-(X)]/PPNX catalysts is the complexity of the polymerization rate law. Reaction orders in [Co(III)] are typically between 1 and 2 and the optimal [PPNCl] loading lies from 0.5 to 2 (vs [Co]).[13−15,29,62] Authors have speculated regarding mono-, dinuclear, and ionic (i.e., off-metal) intermediates and mechanisms to rationalize this data.[13,14,16,17,22,29,45,62−65] Because the ionic cocatalyst performs multiple functions, including nucleophilic attack, coordination, and stabilizing free ionic polymer chains, it is very difficult to design better catalysts.[66]

Given the impressive performance of **2**, particularly as its structure is not yet optimized, it is important to establish its rate law and mechanism. To determine the order in propylene oxide concentration, catalyst **2** was dissolved in a 50:50 mixture of PO:diethyl carbonate (total volume 6 mL) with a resulting PO concentration of 7 M and heated to 50 °C, under 20 bar $CO_2$ pressure. Using a ReactIR instrument the concentration of PO vs time was evaluated and the data plotted. In the early stages of the reaction (0−30% PO conversion), the data shows a sigmoidal decrease in PO concentration, consistent with slow initiation. The semi-logarithmic plot shows a linear relationship ($k_{obs}$ = 3.82 × $10^{-5}$ $s^{-1}$, $R^2$ = 0.9992) indicative of a first order in epoxide concentration (Figure 4a). To determine the order in catalyst concentration, a series of reactions were carried out in neat PO (14 M), 20 bar $CO_2$, at 50 °C using a range of concentrations of catalyst **2** (1.56−7.13 mM) (Table S1). All reactions afforded perfectly alternating PPC, without ether linkages, and without any significant cyclic carbonate (<5%). Plotting the logarithm of the observed rate coefficient vs the logarithm of catalyst concentration shows a linear fit, with a gradient of 0.96 ($R^2$ = 0.9526), indicating a first order in catalyst concentration. The rate dependence on $CO_2$ pressure was determined by measuring the observed rate coefficient ($k_{obs}$) over a range of $CO_2$ pressures from 5 to 30 bar, using 3.57 mM catalyst, neat PO (14 M) and at 50 °C (Table S2). The plot of the rate coefficient versus pressure ($k_{obs}$ vs $P_{CO_2}$) resulted in a slightly curved fit to the data, but without significant rate changes over the range 10−25 bar. Slightly lower rates were observed at 5 bar and this is attributed to the increased formation of cyclic carbonate, perhaps resulting from the relatively low $CO_2$ concentration in solution. At higher $CO_2$ pressures (>20 bar) activity again slightly decreases likely due to gas expansion, prior to the critical point, reducing the overall catalyst and epoxide concentrations.[67] Overall, the reaction is proposed to operate via a second order rate law: first order in both catalyst and epoxide concentrations.

$$\text{Rate} = [\text{Cat}]^1[\text{PO}]^1[\text{CO}_2]^0$$



https://dx.doi.org/10.1021/jacs.0c07980
J. Am. Chem. Soc. 2020, 142, 19150−19160

The kinetic data could be interpreted by a rate-determining step (RDS) involving the ring-opening of the potassium-coordinated epoxide by a cobalt(III)−carbonate intermediate which would be in accordance with a dinuclear mechanism (Figure. 4d, Figure S18). In the solid state complex **2** exhibits a cobaltate structure, i.e., both acetate ligands are coordinated to cobalt (Figure 2b). Accordingly it is hypothesized that propylene oxide (PO) coordination occurs at the oxophilic cationic potassium (Figure S18). In related Ni(II)/Na(I) complexes an internal electric dipole is proposed to localize a positive electric field at Na(I).[55] By analogy, potassium may be electrostatically biased toward epoxide coordination. The mechanistic hypothesis involves propylene oxide coordination being followed by cobaltate acetate nucleophilic attack, during initiation, and by a cobaltate-carbonate intermediate, during propagation. The PO ring-opening results in the formation of a potassium coordinated alkoxide. Carbon dioxide insertion (re)generates the putative cobaltate carbonate intermediate and is proposed as the catalyst resting state. Chain propagation involves both metals and is proposed to occur by a "chain-shuttling" mechanism, akin to $CHO/CO_2$ ROCOP by dinuclear catalysts.[34,36,38,44,45,47,48,65]

To better understand the catalysis, the temperature dependence of rate and selectivity were investigated (Table S3). Polymerizations were conducted from 40 to 70 °C, using [**2**] of 3.57 mM, in neat PO (14 M), at 20 bar $CO_2$ pressure, and using 20 equiv of 1,2-cyclohexane diol. All polymerizations resulted in quantitative carbon dioxide uptake (>99%). Increasing the temperature increased the catalytic activity, from 134 to 834 $h^{-1}$, but the polymer selectivity only slightly decreased. The cyclic carbonate is proposed to form by chain backbiting reactions and these may occur from the alkoxide intermediate. The concentration of the alkoxide intermediate likely increases with temperature due to decreased carbon dioxide solubility. To test this hypothesis, a reaction was conducted at elevated temperature (and otherwise identical conditions) but with a greater $CO_2$ pressure (30 bar): these reaction conditions restore polymer selectivity to >90% while maintaining very high catalytic activity (TOF = 800 $h^{-1}$). All polymerizations resulted in molar mass values consistent with theoretical expectations and in monomodal distributions ($Đ$ < 1.1), i.e., catalyst **2** showed very high control and selectivity for polyol even at higher temperatures. Eyring analysis, i.e., a plot of $\ln(k_p/T)$ versus $1/T$, determined the transition state enthalpy, $\Delta H^{‡}$ = 56.0 ± 1.8 kJ $mol^{-1}$, and entropy, $\Delta S^{‡}$ = −112.7 ± 5.5 J $mol^{-1}$ $K^{-1}$ (Figure 5). Overall, the transition state Gibbs free energy was determined as $\Delta G^{‡}$ = 92.6 ± 2.5 kJ $mol^{-1}$ (50 °C). To compare with ROCOP catalysts, which are often only analyzed by Arrhenius methods (Figure S19), simple activation energy values ($E_a$) were also determined. For PPC formation, **2** shows $E_a$ = 58.9 ± 1.8 kJ $mol^{-1}$. Its activation energy is lower than [(salen)Cr(III)(Cl)]/*N*-MeIm ($E_a$ = 67.6 kJ $mol^{-1}$),[68] but higher than [(salen)Co(X)]/PPNCl or tethered [(salen[$NR_3^+$])$Co(X)_2$], where $E_a$ = 29−35 kJ $mol^{-1}$.[69−71]

Compared to M(II)M′(II) dinuclear catalysts, used in $CHO/CO_2$ ROCOP, it shows significantly lower Gibbs free energy, $\Delta G$ = 95−110 kJ $mol^{-1}$.[40,43] Given the outstanding performance of complex **2** in $PO/CO_2$ ROCOP, it was useful to observe that it was also an excellent catalyst for a range of other epoxides in ROCOP with $CO_2$ (Table 3, Figure S20). In all cases, the same conditions were applied as for $PO/CO_2$ ROCOP: 3.57 mM catalyst, neat epoxide (6 mL), 1,2-cyclohexene diol (71.4 mM), 50 °C, and 20 bar $CO_2$. Catalyst **2** shows impressive activity for most other epoxides and in all cases ensures high carbon dioxide uptake (>99%) without ether linkage formation. In most cases, the selectivity for polymer is very high (>95%) with only trace quantities of cyclic carbonate (<5%). All the polycarbonate polyols show molar mass values consistent with theoretical values and monomodal distributions, with narrow dispersity (>1.30 $Đ$), consistent with well-controlled polymerizations (Figure S21).

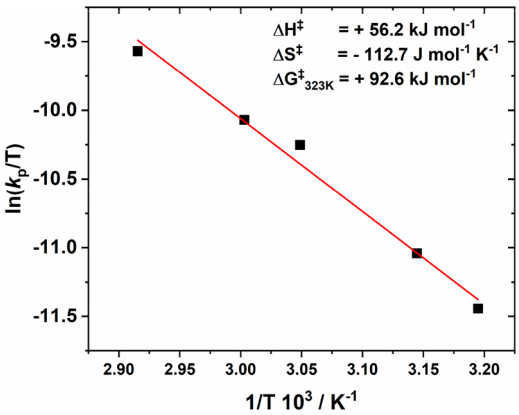


**Figure 5.** Eyring plot, $\ln(k_p/T)$ versus $1/T$, for complex **2** over the temperature range 40−70 °C, 3.57 mM catalyst, neat PO (6 mL), 1,2-cyclohexene diol (71 mmol), under 20 bar $CO_2$ (Table S3).

For example, ROCOP using 2-vinyl oxirane (vPO) is important for postfunctionalization and cross-linking of the resulting polycarbonate.[72−75] Using catalyst **2**, $vPO/CO_2$ ROCOP was slightly slower than for PO, perhaps due to oxirane deactivation by the allyl substituent. There are only a few $vPO/CO_2$ ROCOP catalysts, and compared with these, **2** shows outstanding performances. It shows equivalent activity to the highly optimized quaternary ammonium [(salen)Co(III)($NR_3$)X′)] system (TOF = 40 $h^{-1}$, 0.1 mol % cat, 30 bar $CO_2$, 40 °C).[76,77] This finding demonstrates the significant potential for future improvement to this new class of catalyst, for example, by ligand structure−activity studies. ROCOP using allyl glycidyl ether (AGE) was also successful and illustrates the importance of comparing reactions according to their polymerization rate coefficient ($k_p$). Although the TOF for PO ROCOP appears greater, the $k_p$ for AGE ROCOP is in fact significantly greater (15.4 vs 11.2 $mM^{-1}$ $s^{-1}$). The difference arises because the intrinsic molarity of PO is higher than that of AGE (14.3 M vs 8.4 M). Therefore, after taking into consideration the absolute epoxide concentrations, the ROCOP of $CO_2$/AGE is faster than $CO_2$/PO. This result is important since it demonstrates the potential to produce unsaturated polycarbonates with even greater activity than using PO, thereby providing an efficient future route to polycarbonate amphiphiles or functionalized materials. Co-polymerization of *tert*-butyl glycidyl ether (*t*BGE)/$CO_2$ was about half the activity when using AGE (219 $h^{-1}$ vs 116 $h^{-1}$) with a slight reduction in polymer selectivity (cyclic carbonate = 8 vs >1%). The differences may arise from different steric profiles for the two monomers. Catalysts **2** displays comparable activity to a [(salen)Co(III)($NR_3^+$)$(DNP)_2$] catalyst (119 $h^{-1}$, 0.05 mol %, 40 °C, 15 bar $CO_2$)[78] Reaction of styrene oxide $SO/CO_2$ formed mostly styrene carbonate (91%), presumably because the electron withdrawing phenyl substituent increases the methine carbon's electrophilicity and favors backbiting by


https://dx.doi.org/10.1021/jacs.0c07980
J. Am. Chem. Soc. 2020, 142, 19150−19160

Table 3. Monomer Scope Data for $CO_2$/Epoxide ROCOP Using Catalyst 2[a]

| entry | epoxide | | time (h) | conv. (%)[b] | $CO_2$ (%)[c] | polym. (%)[d] | TON[e] | TOF ($h^{-1}$)[f] | $k_p$ ($mM^{-1}$ $s^{-1}$)[g] | $M_n$ [$Đ$] (g $mol^{-1}$)[h] |
|---|---|---|---|---|---|---|---|---|---|---|
| 1 | Acyclic | PO | 4.2 | 34 | >99 | >99 | 1352 | 340 | 11.2 | 5900 [1.10] |
| 2 | | vPO | 23.5 | 60 | >99 | >99 | 2091 | 89 | 5.9 | 4100 [1.30] |
| 3 | | AGE | 5.6 | 51 | >99 | >99 | 1220 | 219 | 15.4 | 3900 [1.28] |
| 4 | | $^t$BGE | 7.9 | 46 | >99 | 92 | 908 | 116 | 7.4 | 5100 [1.15] |
| 5 | | SO | 22.3 | 21 | >99 | 9 | 511 | 23 | n.a. | n.a. |
| 6 | Cyclic | CHO | 2.3 | 52 | >99 | >99 | 1430 | 631 | 31.7 | 5900 [1.10] |
| 7 | | vCHO | 3.2 | 60 | >99 | >99 | 1285 | 408 | 24.6 | 9500 [1.08] |
| 8 | | CPO | 6.3 | 32 | >99 | 95 | 1062 | 162 | 5.1 | 4200 [1.07] |

[a]Reaction conditions: Catalyst 2 (3.57 mM), neat epoxide (6 mL), 1,2-cyclohexane diol (20 equiv vs 2), 20 bar $CO_2$ and 50 °C. [b]Epoxide conversion determined by comparison of the relative integrals in the $^1$H NMR spectrum of PC, CC, and PE against mesitylene (6.59 ppm, 10 equiv). [c]$CO_2$ selectivity determined by comparison of the relative integrals in the $^1$H NMR spectrum for PC and CC against PE. [d]Polymer selectivity determined by comparison of the relative integrals in the $^1$H NMR spectrum for PC against CC. [e]Turnover number (TON) = number of moles of epoxide consumed/number of moles catalyst. [f]Turnover frequency (TOF) = TON/time (h). [g]$k_p = k_{obs}/[cat]^1$; $k_{obs}$ determined as the gradient of the plot of $\ln([Epoxide]_t/[Epoxide]_0)$ vs time, [2] = 3.57 mM. [h]GPC analysis, in THF, calibrated using narrow-$M_n$ polystyrene standards, dispersity values in parentheses. Note that Figure S22 illustrates the leading literature catalysts for each epoxide.

the nucleophilic carbonate/alkoxide intermediates. Darensbourg and co-workers applied [(salen)Co(III)(X)]/PPNCl catalysts for $CO_2$/SO ROCOP and noted that only X= DNP (2,4-dinitrophenolate) performed effectively (X = DNP 90%; Cl = 58%; and Br = 5% PPC formation).[79]

In the future it may be possible to improve the selectivity of catalyst 2 for polycarbonate by changing the acetate ligand or by substituting 1,2-cyclohexene diol for 1-phenyl-1,2-ethanediol as the chain transfer agent. Cyclic epoxides generally proceeded with a higher rate constant ($k_p$) than acyclic epoxides (Table 2). The release of ring-strain provides an additional driving force, and 6-membered ring epoxides, e.g., cyclohexene oxide (CHO) or vinyl-cyclohexene oxide (vCHO), are usually polymerized significantly faster than 5-membered ring epoxides, such as cyclopentene oxide (CPO). Catalyst 2 was highly active for $CO_2$/CHO ROCOP and showed a polymerization rate constant more than double that of a previous high performance [Mg(II)Co(II)] heterodinuclear catalyst (2, $k_p$ = 31.7 $mM^{-1}$ $s^{-1}$ (50 °C) versus [Co(II)Mg(II)], $k_p$ = 15.1 $mM^{-1}$ $s^{-1}$(60 °C))[43] and achieves comparable activity to the quaternary ammonium cobalt catalyst systems (TOF = 1018 $h^{-1}$, catalyst = 0.02 mol %, 50 °C, 20 bar $CO_2$).[80] Its overall performance in CHO/$CO_2$ ROCOP is better than the widely investigated $\beta$-diiminate di-Zn-catalyst (TOF = 2290 $h^{-1}$, 50 °C, 0.1 mol % cat, 69 bar $CO_2$, 90% PCHC formation), as it is applied at 4× lower catalyst loading.[81] It is significantly less active than the tethered $\beta$-diiminate di-Zn catalysts, reported by Rieger and co-workers, which delivers poly(cyclohexene carbonate) with ∼80% carbonate linkages only (155 000 $h^{-1}$, 0.0125 mol %, 100 °C, 30 bar $CO_2$) although 2 is tested at significantly lower temperature preventing easy comparison.[82] It is also important to note that these optimized di-Zn catalysts show negligible activity for propylene oxide/carbon dioxide copolymerization (1 $h^{-1}$, 0.025 mol %, 60 °C, 23% polymer).[83]

ROCOP using functionalized vinyl-cyclohexene oxide (vCHO)/$CO_2$ is also highly active and selective; the product polycarbonate undergoes postfunctionalization, cross-linking and network formation.[84,85] The $CO_2$/cyclopentene oxide (CPO) ROCOP forms a polycarbonate which under certain conditions can be depolymerized to epoxide, rather than to cyclic carbonate, thus providing a future chemical recycling route.[86,87] Using catalyst 2 for the ROCOP of CPO/$CO_2$ resulted in polycarbonate formation with excellent selectivity (95%) (Table 2, Entry 8). The catalytic activity is high, TOF = 162 $h^{-1}$, particularly given the low catalyst loading applied (0.025 mol % cat, 50 °C, 20 bar $CO_2$, neat CPO). Indeed the activity of 2 is four times higher than the most active cobalt-salen derivative which is applied at four times higher loading (TOF = 42 $h^{-1}$, 0.1 mol % cat, 50 °C, 20 bar $CO_2$).[88] It is also double the activity of a chromium-salen derivative, again applied at four times higher loading than 2, (TOF = 77 $h^{-1}$, 0.1 mol % cat, 70 °C, 20 bar $CO_2$).[88] Overall, the heterodinuclear Co(III)/K(I) catalyst shows outstanding performance using a range of other epoxides in alternating copolymerizations with carbon dioxide. We plan to continue to optimize the ligand and metal selection so as to further increase performances.

## CONCLUSION

In conclusion, a new class of heterodinuclear Co(III)/M(I) complexes were highly active, selective, and controlled catalysts for propylene oxide/carbon dioxide ring-opening copolymerizations. The complexes demonstrate the power of asymmetrical macrocycle ligands to bias the coordination chemistry and reactivity to deliver highly effective catalysis. These complexes have significant potential for future optimization, including through modifications of the substituents, metal combinations, and coligand chemistries. Since this is the first demonstration of how to exploit Group 1 metals in this catalysis, further investigation into the power of these inexpensive, colorless, and abundant metals for carbon dioxide utilization catalysis is certainly warranted. Group 1 metals offer tremendous potential in terms of operability and scale-up, and the Co(III)/K(I) catalyst challenged the performance of the status-quo tethered catalyst systems which rely on expensive salts, like PPNCl. The best catalyst, Co(III)/K(I), delivered high polymerization conversions, excellent activity, and an impressive operating temperature window (25−70 °C). The activity reached values of TOF = 800 $h^{-1}$, and it was applied at useful, low loading (0.025 mol %). It was also highly active for a range of other epoxides, including those substituted with alkene groups. Kinetic analyses showed an overall second order rate law and implicate a chain shuttling dinuclear mechanism. The catalysts warrant future investigation for related polymerizations, such as lactone ring-opening polymerizations, switch polymerization catalysis, and epoxide/anhydride ROCOP. The beneficial combination of Co(III) and Group 1 metals could also accelerate other carbon dioxide, and heterocumulene,


https://dx.doi.org/10.1021/jacs.0c07980
J. Am. Chem. Soc. 2020, 142, 19150−19160

transformations, including production of heterocycles, N-containing polymers, polyesters, and even carbon dioxide reduction products.

## ■ ASSOCIATED CONTENT

### Supporting Information

The Supporting Information is available free of charge at https://pubs.acs.org/doi/10.1021/jacs.0c07980.

Characterization data of catalysts (1D and 2D NMR spectroscopy, mass spectrometry, infrared spectroscopy, and X-ray crystallography); Polymerization kinetics and characterization (NMR spectroscopy and gel permeation chromatograms) (PDF)

Crystal data (CIF)

## ■ AUTHOR INFORMATION


### Corresponding Author

**Charlotte K. Williams** − *Department of Chemistry, Chemistry Research Laboratory, University of Oxford, Oxford OX1 3TA, U.K.*; orcid.org/0000-0002-0734-1575; Email: charlotte.williams@chem.ox.ac.uk

### Authors

**Arron C. Deacy** − *Department of Chemistry, Chemistry Research Laboratory, University of Oxford, Oxford OX1 3TA, U.K.*

**Emma Moreby** − *Department of Chemistry, Chemistry Research Laboratory, University of Oxford, Oxford OX1 3TA, U.K.*

**Andreas Phanopoulos** − *Department of Chemistry, Chemistry Research Laboratory, University of Oxford, Oxford OX1 3TA, U.K.*

Complete contact information is available at: https://pubs.acs.org/10.1021/jacs.0c07980


### Notes

The authors declare the following competing financial interest(s): CKW is a director of Econic Technologies, Ltd.

## ■ ACKNOWLEDGMENTS

The Engineering and Physical Sciences Research Council (EP/S018603/1; EP/R027129/1) and the Oxford Martin School (Future of Plastics) are acknowledged for research funding.

## ■ REFERENCES


(1) Burkart, M. D.; Hazari, N.; Tway, C. L.; Zeitler, E. L. Opportunities and Challenges for Catalysis in Carbon Dioxide Utilization. *ACS Catal.* **2019**, *9* (9), 7937−7956.

(2) Artz, J.; Müller, T. E.; Thenert, K.; Kleinekorte, J.; Meys, R.; Sternberg, A.; Bardow, A.; Leitner, W. Sustainable Conversion of Carbon Dioxide: An Integrated Review of Catalysis and Life Cycle Assessment. *Chem. Rev.* **2018**, *118* (2), 434−504.

(3) Hepburn, C.; Adlen, E.; Beddington, J.; Carter, E. A.; Fuss, S.; Mac Dowell, N.; Minx, J. C.; Smith, P.; Williams, C. K. The technological and economic prospects for $CO_2$ utilization and removal. *Nature* **2019**, *575* (7781), 87−97.

(4) Darensbourg, D. J. Chain transfer agents utilized in epoxide and $CO_2$ copolymerization processes. *Green Chem.* **2019**, *21* (9), 2214−2223.

(5) Wang, Y.; Darensbourg, D. J. Carbon dioxide-based functional polycarbonates: Metal catalyzed copolymerization of $CO_2$ and epoxides. *Coord. Chem. Rev.* **2018**, *372*, 85−100.

(6) Alagi, P.; Ghorpade, R.; Choi, Y. J.; Patil, U.; Kim, I.; Baik, J. H.; Hong, S. C. Carbon Dioxide-Based Polyols as Sustainable Feedstock of Thermoplastic Polyurethane for Corrosion-Resistant Metal Coating. *ACS Sustainable Chem. Eng.* **2017**, *5* (5), 3871−3881.

(7) Langanke, J.; Wolf, A.; Hofmann, J.; Bohm, K.; Subhani, M. A.; Muller, T. E.; Leitner, W.; Gurtler, C. Carbon dioxide ($CO_2$) as sustainable feedstock for polyurethane production. *Green Chem.* **2014**, *16* (4), 1865−1870.

(8) Lee, S. H.; Cyriac, A.; Jeon, J. Y.; Lee, B. Y. Preparation of thermoplastic polyurethanes using in situ generated poly(propylene carbonate)-diols. *Polym. Chem.* **2012**, *3* (5), 1215−1220.

(9) von der Assen, N.; Bardow, A. Life cycle assessment of polyols for polyurethane production using $CO_2$ as feedstock: insights from an industrial case study. *Green Chem.* **2014**, *16* (6), 3272−3280.

(10) Sulley, G. S.; Gregory, G. L.; Chen, T. T. D.; Peña Carrodeguas, L.; Trott, G.; Santmarti, A.; Lee, K.-Y.; Terrill, N. J.; Williams, C. K. Switchable Catalysis Improves the Properties of $CO_2$-Derived Polymers: Poly(cyclohexene carbonate-b-$\varepsilon$-decalactone-b-cyclohexene carbonate) Adhesives, Elastomers, and Toughened Plastics. *J. Am. Chem. Soc.* **2020**, *142* (9), 4367−4378.

(11) Leow, W. R.; Lum, Y.; Ozden, A.; Wang, Y.; Nam, D.-H.; Chen, B.; Wicks, J.; Zhuang, T.-T.; Li, F.; Sinton, D.; Sargent, E. H. Chloride-mediated selective electrosynthesis of ethylene and propylene oxides at high current density. *Science* **2020**, *368* (6496), 1228−1233.

(12) Lu, X. B.; Ren, W. M.; Wu, G. P. $CO_2$ Copolymers from Epoxides: Catalyst Activity, Product Selectivity, and Stereochemistry Control. *Acc. Chem. Res.* **2012**, *45* (10), 1721−1735.

(13) Lu, X. B.; Shi, L.; Wang, Y. M.; Zhang, R.; Zhang, Y. J.; Peng, X. J.; Zhang, Z. C.; Li, B. Design of highly active binary catalyst systems for $CO_2$/epoxide copolymerization: Polymer selectivity, enantioselectivity, and stereochemistry control. *J. Am. Chem. Soc.* **2006**, *128* (5), 1664−1674.

(14) Liu, J.; Ren, W. M.; Liu, Y.; Lu, X. B. Kinetic Study on the Coupling of $CO_2$ and Epoxides Catalyzed by Co(III) Complex with an Inter- or Intramolecular Nucleophilic Cocatalyst. *Macromolecules* **2013**, *46* (4), 1343−1349.

(15) Noh, E. K.; Na, S. J.; Sujith, S.; Kim, S. W.; Lee, B. Y. Two components in a molecule: Highly efficient and thermally robust catalytic system for $CO_2$/Epoxide copolymerization. *J. Am. Chem. Soc.* **2007**, *129* (26), 8082−8083.

(16) Nakano, K.; Kobayashi, K.; Nozaki, K. Tetravalent Metal Complexes as a New Family of Catalysts for Copolymerization of Epoxides with Carbon Dioxide. *J. Am. Chem. Soc.* **2011**, *133* (28), 10720−10723.

(17) Nakano, K.; Hashimoto, S.; Nozaki, K. Bimetallic mechanism operating in the copolymerization of propylene oxide with carbon dioxide catalyzed by cobalt-salen complexes. *Chem. Sci.* **2010**, *1* (3), 369−373.

(18) Nakano, K.; Kamada, T.; Nozaki, K. Selective formation of polycarbonate over cyclic carbonate: Copolymerization of epoxides with carbon dioxide catalyzed by a cobalt(III) complex with a piperidinium end-capping arm. *Angew. Chem., Int. Ed.* **2006**, *45* (43), 7274−7277.

(19) Cohen, C. T.; Chu, T.; Coates, G. W. Cobalt catalysts for the alternating copolymerization of propylene oxide and carbon dioxide: Combining high activity and selectivity. *J. Am. Chem. Soc.* **2005**, *127* (31), 10869−10878.

(20) Qin, Z. Q.; Thomas, C. M.; Lee, S.; Coates, G. W. Cobalt-based complexes for the copolymerization of propylene oxide and CO2: Active and selective catalysts for polycarbonate synthesis. *Angew. Chem., Int. Ed.* **2003**, *42* (44), 5484−5487.

(21) Allen, S. D.; Moore, D. R.; Lobkovsky, E. B.; Coates, G. W. High-activity, single-site catalysts for the alternating copolymerization of CO2 and propylene oxide. *J. Am. Chem. Soc.* **2002**, *124* (48), 14284−14285.

(22) Vagin, S. I.; Reichardt, R.; Klaus, S.; Rieger, B. Conformationally Flexible Dimeric Salphen Complexes for Bifunctional Catalysis. *J. Am. Chem. Soc.* **2010**, *132* (41), 14367−14369.

(23) Zhang, D. Y.; Boopathi, S. K.; Hadjichristidis, N.; Gnanou, Y.; Feng, X. S. Metal-Free Alternating Copolymerization of CO2 with

Epoxides: Fulfilling "Green" Synthesis and Activity. *J. Am. Chem. Soc.* **2016**, *138* (35), 11117−11120.
(24) Jia, M. C.; Hadjichristidis, N.; Gnanou, Y.; Feng, X. S. Monomodal Ultrahigh-Molar-Mass Polycarbonate Homopolymers and Diblock Copolymers by Anionic Copolymerization of Epoxides with CO2. *ACS Macro Lett.* **2019**, *8* (12), 1594−1598.
(25) Wu, G.-P.; Darensbourg, D. J. Mechanistic Insights into Water-Mediated Tandem Catalysis of Metal-Coordination $CO_2$/Epoxide Copolymerization and Organocatalytic Ring-Opening Polymerization: One-Pot, Two Steps, and Three Catalysis Cycles for Triblock Copolymers Synthesis. *Macromolecules* **2016**, *49* (3), 807−814.
(26) Darensbourg, D. J.; Wu, G. P. A One-Pot Synthesis of a Triblock Copolymer from Propylene Oxide/Carbon Dioxide and Lactide: Intermediacy of Polyol Initiators. *Angew. Chem., Int. Ed.* **2013**, *52* (40), 10602−10606.
(27) Cyriac, A.; Lee, S. H.; Varghese, J. K.; Park, E. S.; Park, J. H.; Lee, B. Y. Immortal CO2/Propylene Oxide Copolymerization: Precise Control of Molecular Weight and Architecture of Various Block Copolymers. *Macromolecules* **2010**, *43* (18), 7398−7401.
(28) Yoo, J.; Na, S. J.; Park, H. C.; Cyriac, A.; Lee, B. Y. Anion variation on a cobalt(iii) complex of salen-type ligand tethered by four quaternary ammonium salts for CO2/epoxide copolymerization. *Dalton Trans.* **2010**, *39* (10), 2622−2630.
(29) Na, S. J.; Sujith, S.; Cyriac, A.; Kim, B. E.; Yoo, J.; Kang, Y. K.; Han, S. J.; Lee, C.; Lee, B. Y. Elucidation of the Structure of a Highly Active Catalytic System for CO2/Epoxide Copolymerization: A salen-Cobaltate Complex of an Unusual Binding Mode. *Inorg. Chem.* **2009**, *48* (21), 10455−10465.
(30) Deng, J.; Ratanasak, M.; Sako, Y.; Tokuda, H.; Maeda, C.; Hasegawa, J.-y.; Nozaki, K.; Ema, T. Aluminum porphyrins with quaternary ammonium halides as catalysts for copolymerization of cyclohexene oxide and CO2: metal−ligand cooperative catalysis. *Chem. Sci.* **2020**, *11* (22), 5669−5675.
(31) Patil, N. G.; Boopathi, S. K.; Alagi, P.; Hadjichristidis, N.; Gnanou, Y.; Feng, X. Carboxylate Salts as Ideal Initiators for the Metal-Free Copolymerization of CO2 with Epoxides: Synthesis of Well-Defined Polycarbonates Diols and Polyols. *Macromolecules* **2019**, *52* (6), 2431−2438.
(32) Patil, N.; Bhoopathi, S.; Chidara, V.; Hadjichristidis, N.; Gnanou, Y.; Feng, X. Recycling a Borate Complex for Synthesis of Polycarbonate Polyols: Towards an Environmentally Friendly and Cost-Effective Process. *ChemSusChem* **2020**, *13* (18), 5080−5087.
(33) Yang, G.-W.; Zhang, Y.-Y.; Xie, R.; Wu, G.-P. Scalable Bifunctional Organoboron Catalysts for Copolymerization of CO2 and Epoxides with Unprecedented Efficiency. *J. Am. Chem. Soc.* **2020**, *142*, 12245.
(34) Trott, G.; Garden, J. A.; Williams, C. K. Heterodinuclear zinc and magnesium catalysts for epoxide/CO2 ring opening copolymerizations. *Chem. Sci.* **2019**, *10* (17), 4618−4627.
(35) Deacy, A. C.; Durr, C. B.; Garden, J. A.; White, A. J. P.; Williams, C. K. Groups 1, 2 and Zn(II) Heterodinuclear Catalysts for Epoxide/CO2 Ring-Opening Copolymerization. *Inorg. Chem.* **2018**, *57* (24), 15575−15583.
(36) Garden, J. A.; Saini, P. K.; Williams, C. K. Greater than the Sum of Its Parts: A Heterodinuclear Polymerization Catalyst. *J. Am. Chem. Soc.* **2015**, *137* (48), 15078−15081.
(37) Chapman, A. M.; Keyworth, C.; Kember, M. R.; Lennox, A. J. J.; Williams, C. K. Adding Value to Power Station Captured CO2: Tolerant Zn and Mg Homogeneous Catalysts for Polycarbonate Polyol Production. *ACS Catal.* **2015**, *5* (3), 1581−1588.
(38) Saini, P. K.; Romain, C.; Williams, C. K. Dinuclear metal catalysts: improved performance of heterodinuclear mixed catalysts for $CO_2$-epoxide copolymerization. *Chem. Commun.* **2014**, *50* (32), 4164−4167.
(39) Kember, M. R.; Williams, C. K. Efficient Magnesium Catalysts for the Copolymerization of Epoxides and $CO_2$; Using Water to Synthesize Polycarbonate Polyols. *J. Am. Chem. Soc.* **2012**, *134* (38), 15676−15679.
(40) Jutz, F.; Buchard, A.; Kember, M. R.; Fredriksen, S. B.; Williams, C. K. Mechanistic Investigation and Reaction Kinetics of the Low-Pressure Copolymerization of Cyclohexene Oxide and Carbon Dioxide Catalyzed by a Dizinc Complex. *J. Am. Chem. Soc.* **2011**, *133* (43), 17395−17405.
(41) Buchard, A.; Kember, M. R.; Sandeman, K. G.; Williams, C. K. A bimetallic iron(III) catalyst for $CO_2$/epoxide coupling. *Chem. Commun.* **2011**, *47* (1), 212−214.
(42) Kember, M. R.; Knight, P. D.; Reung, P. T. R.; Williams, C. K. Highly Active Dizinc Catalyst for the Copolymerization of Carbon Dioxide and Cyclohexene Oxide at One Atmosphere Pressure. *Angew. Chem., Int. Ed.* **2009**, *48* (5), 931−933.
(43) Deacy, A. C.; Kilpatrick, A. F. R.; Regoutz, A.; Williams, C. K. Understanding metal synergy in heterodinuclear catalysts for the copolymerization of CO2 and epoxides. *Nat. Chem.* **2020**, *12* (4), 372−380.
(44) Trott, G.; Saini, P. K.; Williams, C. K. Catalysts for $CO_2$/Epoxide Ring-Opening Copolymerization. *Philos. Trans. R. Soc., A* **2016**, *374* (2061), 20150085.
(45) Buchard, A.; Jutz, F.; Kember, M. R.; White, A. J. P.; Rzepa, H. S.; Williams, C. K. Experimental and Computational Investigation of the Mechanism of Carbon Dioxide/Cyclohexene Oxide Copolymerization Using a Dizinc Catalyst. *Macromolecules* **2012**, *45* (17), 6781−6795.
(46) Kember, M. R.; White, A. J. P.; Williams, C. K. Highly Active Di- and Trimetallic Cobalt Catalysts for the Copolymerization of CHO and $CO_2$ at Atmospheric Pressure. *Macromolecules* **2010**, *43* (5), 2291−2298.
(47) Asaba, H.; Iwasaki, T.; Hatazawa, M.; Deng, J.; Nagae, H.; Mashima, K.; Nozaki, K. Alternating Copolymerization of CO2 and Cyclohexene Oxide Catalyzed by Cobalt−Lanthanide Mixed Multinuclear Complexes. *Inorg. Chem.* **2020**, *59* (12), 7928−7933.
(48) Nagae, H.; Aoki, R.; Akutagawa, S.; Kleemann, J.; Tagawa, R.; Schindler, T.; Choi, G.; Spaniol, T. P.; Tsurugi, H.; Okuda, J.; Mashima, K. Lanthanide Complexes Supported by a Trizinc Crown Ether as Catalysts for Alternating Copolymerization of Epoxide and $CO_2$: Telomerization Controlled by Carboxylate Anions. *Angew. Chem., Int. Ed.* **2018**, *57* (9), 2492−2496.
(49) Deacy, A. C.; Durr, C. B.; Williams, C. K. Heterodinuclear complexes featuring Zn(ii) and M = Al(iii), Ga(iii) or In(iii) for cyclohexene oxide and CO2 copolymerisation. *Dalton Trans.* **2020**, *49* (1), 223−231.
(50) Klaus, S.; Lehenmeier, M. W.; Herdtweck, E.; Deglmann, P.; Ott, A. K.; Rieger, B. Mechanistic Insights into Heterogeneous Zinc Dicarboxylates and Theoretical Considerations for CO2−Epoxide Copolymerization. *J. Am. Chem. Soc.* **2011**, *133* (33), 13151−13161.
(51) Du, K.; Thorarinsdottir, A. E.; Harris, T. D. Selective Binding and Quantitation of Calcium with a Cobalt-Based Magnetic Resonance Probe. *J. Am. Chem. Soc.* **2019**, *141* (17), 7163−7172.
(52) Chantarojsiri, T.; Ziller, J. W.; Yang, J. Y. Incorporation of redox-inactive cations promotes iron catalyzed aerobic C−H oxidation at mild potentials. *Chem. Sci.* **2018**, *9* (9), 2567−2574.
(53) Martinez, A.; Hemmert, C.; Gornitzka, H.; Meunier, B. Synthesis and activity of macrocyclized chiral Mn(III)−Schiff-base epoxidation catalysts. *J. Organomet. Chem.* **2005**, *690* (9), 2163−2171.
(54) Reath, A. H.; Ziller, J. W.; Tsay, C.; Ryan, A. J.; Yang, J. Y. Redox Potential and Electronic Structure Effects of Proximal Nonredox Active Cations in Cobalt Schiff Base Complexes. *Inorg. Chem.* **2017**, *56* (6), 3713−3718.
(55) Kang, K.; Fuller, J.; Reath, A. H.; Ziller, J. W.; Alexandrova, A. N.; Yang, J. Y. Installation of internal electric fields by non-redox active cations in transition metal complexes. *Chem. Sci.* **2019**, *10* (43), 10135−10142.
(56) Chantarojsiri, T.; Reath, A. H.; Yang, J. Y. Cationic Charges Leading to an Inverse Free-Energy Relationship for N−N Bond Formation by MnVI Nitrides. *Angew. Chem., Int. Ed.* **2018**, *57* (43), 14037−14042.
(57) Rollinson, H.; Adetunji, J. Ionic Radii. In *Encyclopedia of Geochemistry: A Comprehensive Reference Source on the Chemistry of the*


https://dx.doi.org/10.1021/jacs.0c07980
J. Am. Chem. Soc. 2020, 142, 19150−19160

*Earth*; White, W. M., Ed.; Springer International Publishing: Cham, 2018; pp 738−743.
(58) Akine, S.; Utsuno, F.; Piao, S.; Orita, H.; Tsuzuki, S.; Nabeshima, T. Synthesis, Ion Recognition Ability, and Metal-Assisted Aggregation Behavior of Dinuclear Metallohosts Having a Bis(Saloph) Macrocyclic Ligand. *Inorg. Chem.* **2016**, *55* (2), 810−821.
(59) Gao, Y.; Gu, L.; Qin, Y.; Wang, X.; Wang, F. Dicarboxylic acid promoted immortal copolymerization for controllable synthesis of low-molecular weight oligo(carbonate-ether) diols with tunable carbonate unit content. *J. Polym. Sci., Part A: Polym. Chem.* **2012**, *50* (24), 5177−5184.
(60) Hinz, W.; Wildeson, J.; Dexheimer, E. M.; Neff, R. Formation of polymer polyols with a narrow polydispersity using double metal cyanide (DMC) catalysts. US6713599B1, 2006.
(61) Gürtler, C.; Hofmann, J.; Wolf, A.; Grasser, S. Method for producing polyether carbonate polyols. US20130123532A1, 2013.
(62) Ohkawara, T.; Suzuki, K.; Nakano, K.; Mori, S.; Nozaki, K. Facile Estimation of Catalytic Activity and Selectivities in Copolymerization of Propylene Oxide with Carbon Dioxide Mediated by Metal Complexes with Planar Tetradentate Ligand. *J. Am. Chem. Soc.* **2014**, *136* (30), 10728−10735.
(63) Darensbourg, D. J.; Fitch, S. B. Copolymerization of Epoxides and Carbon Dioxide. Evidence Supporting the Lack of Dual Catalysis at a Single Metal Site. *Inorg. Chem.* **2009**, *48* (18), 8668−8677.
(64) Darensbourg, D. J. Making Plastics from Carbon Dioxide: Salen Metal Complexes as Catalysts for the Production of Polycarbonates from Epoxides and $CO_2$. *Chem. Rev.* **2007**, *107* (6), 2388−2410.
(65) Liu, Y.; Ren, W.-M.; Liu, C.; Fu, S.; Wang, M.; He, K.-K.; Li, R.-R.; Zhang, R.; Lu, X.-B. Mechanistic Understanding of Dinuclear Cobalt(III) Complex Mediated Highly Enantioselective Copolymerization of meso-Epoxides with CO2. *Macromolecules* **2014**, *47* (22), 7775−7788.
(66) Romain, C.; Thevenon, A.; Saini, P. K.; Williams, C. K., Dinuclear Metal Complex-Mediated Formation of $CO_2$-Based Polycarbonates. In *Carbon Dioxide and Organometallics*; Lu, X. B., Ed.; Springer, 2016; Vol. *53*, pp 101−141.
(67) Mang, S.; Cooper, A. I.; Colclough, M. E.; Chauhan, N.; Holmes, A. B. Copolymerization of CO2 and 1,2-Cyclohexene Oxide Using a CO2-Soluble Chromium Porphyrin Catalyst. *Macromolecules* **2000**, *33* (2), 303−308.
(68) Darensbourg, D. J.; Yarbrough, J. C.; Ortiz, C.; Fang, C. C. Comparative Kinetic Studies of the Copolymerization of Cyclohexene Oxide and Propylene Oxide with Carbon Dioxide in the Presence of Chromium Salen Derivatives. In Situ FTIR Measurements of Copolymer vs Cyclic Carbonate Production. *J. Am. Chem. Soc.* **2003**, *125* (25), 7586−7591.
(69) Wu, G.-P.; Wei, S.-H.; Ren, W.-M.; Lu, X.-B.; Xu, T.-Q.; Darensbourg, D. J. Perfectly Alternating Copolymerization of CO2 and Epichlorohydrin Using Cobalt(III)-Based Catalyst Systems. *J. Am. Chem. Soc.* **2011**, *133* (38), 15191−15199.
(70) Liu, J.; Ren, W.-M.; Liu, Y.; Lu, X.-B. Kinetic Study on the Coupling of CO2 and Epoxides Catalyzed by Co(III) Complex with an Inter- or Intramolecular Nucleophilic Cocatalyst. *Macromolecules* **2013**, *46* (4), 1343−1349.
(71) Chukanova, O. M.; Bukhovets, E. V.; Perepelitsina, E. O.; Belov, G. P. The kinetics of carbon dioxide and propylene oxide copolymerization catalyzed by binary catalyst system. *Polym. Sci., Ser. B* **2015**, *57* (3), 224−227.
(72) Darensbourg, D. J.; Wang, Y. Terpolymerization of propylene oxide and vinyl oxides with CO2: copolymer cross-linking and surface modification via thiol−ene click chemistry. *Polym. Chem.* **2015**, *6* (10), 1768−1776.
(73) Scharfenberg, M.; Hilf, J.; Frey, H. Functional Polycarbonates from Carbon Dioxide and Tailored Epoxide Monomers: Degradable Materials and Their Application Potential. *Adv. Funct. Mater.* **2018**, *28* (10), 16.
(74) Yi, N.; Chen, T. T. D.; Unruangsri, J.; Zhu, Y.; Williams, C. K. Orthogonal functionalization of alternating polyesters: selective patterning of (AB)n sequences. *Chem. Sci.* **2019**, *10* (43), 9974−9980.
(75) Darensbourg, D. J.; Chung, W.-C.; Arp, C. J.; Tsai, F.-T.; Kyran, S. J. Copolymerization and Cycloaddition Products Derived from Coupling Reactions of 1,2-Epoxy-4-cyclohexene and Carbon Dioxide. Postpolymerization Functionalization via Thiol−Ene Click Reactions. *Macromolecules* **2014**, *47* (21), 7347−7353.
(76) Darensbourg, D. J.; Tsai, F.-T. Postpolymerization Functionalization of Copolymers Produced from Carbon Dioxide and 2-Vinyloxirane: Amphiphilic/Water-Soluble CO2-Based Polycarbonates. *Macromolecules* **2014**, *47* (12), 3806−3813.
(77) Chen, K.; Shi, G.; Li, H.; Wang, C.; Darensbourg, D. J. Design of Betaine Functional Catalyst for Efficient Copolymerization of Oxirane and CO2. *Macromolecules* **2018**, *51* (15), 6057−6062.
(78) Konieczynska, M. D.; Lin, X.; Zhang, H.; Grinstaff, M. W. Synthesis of Aliphatic Poly(ether 1,2-glycerol carbonate)s via Copolymerization of CO2 with Glycidyl Ethers Using a Cobalt Salen Catalyst and Study of a Thermally Stable Solid Polymer Electrolyte. *ACS Macro Lett.* **2015**, *4* (5), 533−537.
(79) Wu, G.-P.; Wei, S.-H.; Lu, X.-B.; Ren, W.-M.; Darensbourg, D. J. Highly Selective Synthesis of CO2 Copolymer from Styrene Oxide. *Macromolecules* **2010**, *43* (21), 9202−9204.
(80) Ren, W.-M.; Zhang, X.; Liu, Y.; Li, J.-F.; Wang, H.; Lu, X.-B. Highly Active, Bifunctional Co(III)-Salen Catalyst for Alternating Copolymerization of CO2 with Cyclohexene Oxide and Terpolymerization with Aliphatic Epoxides. *Macromolecules* **2010**, *43* (3), 1396−1402.
(81) Moore, D. R.; Cheng, M.; Lobkovsky, E. B.; Coates, G. W. Electronic and Steric Effects on Catalysts for CO2/Epoxide Polymerization: Subtle Modifications Resulting in Superior Activities. *Angew. Chem., Int. Ed.* **2002**, *41* (14), 2599−2602.
(82) Kissling, S.; Lehenmeier, M. W.; Altenbuchner, P. T.; Kronast, A.; Reiter, M.; Deglmann, P.; Seemann, U. B.; Rieger, B. Dinuclear zinc catalysts with unprecedented activities for the copolymerization of cyclohexene oxide and CO2. *Chem. Commun.* **2015**, *51* (22), 4579−4582.
(83) Kissling, S.; Altenbuchner, P. T.; Lehenmeier, M. W.; Herdtweck, E.; Deglmann, P.; Seemann, U. B.; Rieger, B. Mechanistic Aspects of a Highly Active Dinuclear Zinc Catalyst for the Copolymerization of Epoxides and CO2. *Chem. - Eur. J.* **2015**, *21* (22), 8148−8157.
(84) Wang, Y. Y.; Darensbourg, D. J. Carbon dioxide-based functional polycarbonates: Metal catalyzed copolymerization of CO2 and epoxides. *Coord. Chem. Rev.* **2018**, *372*, 85−100.
(85) Chen, T. T. D.; Zhu, Y.; Williams, C. K. Pentablock Copolymer from Tetracomponent Monomer Mixture Using a Switchable Dizinc Catalyst. *Macromolecules* **2018**, *51* (14), 5346−5351.
(86) Darensbourg, D. J.; Wei, S.-H.; Yeung, A. D.; Ellis, W. C. An Efficient Method of Depolymerization of Poly(cyclopentene carbonate) to Its Comonomers: Cyclopentene Oxide and Carbon Dioxide. *Macromolecules* **2013**, *46* (15), 5850−5855.
(87) Darensbourg, D. J.; Yeung, A. D.; Wei, S.-H. Base initiated depolymerization of polycarbonates to epoxide and carbon dioxide co-monomers: a computational study. *Green Chem.* **2013**, *15* (6), 1578−1583.
(88) Darensbourg, D. J.; Chung, W.-C.; Wilson, S. J. Catalytic Coupling of Cyclopentene Oxide and CO2 Utilizing Bifunctional (salen)Co(III) and (salen)Cr(III) Catalysts: Comparative Processes Involving Binary (salen)Cr(III) Analogs. *ACS Catal.* **2013**, *3* (12), 3050−3057.


https://dx.doi.org/10.1021/jacs.0c07980
*J. Am. Chem. Soc.* 2020, 142, 19150−19160